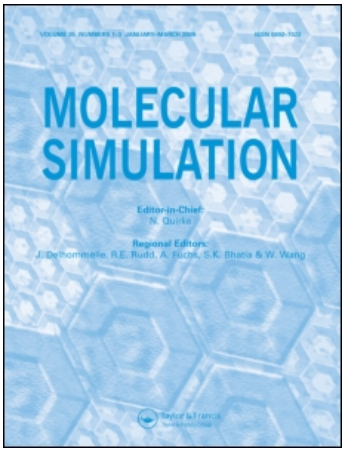

Molecular Simulation
Publication details, including instructions for authors and subscription information:
http://www.informaworld.com/smpp/title~content=t713644482

Docking and binding mode analysis of aryl diketoacids (ADK) at the active site of HCV RNA-dependent RNA polymerase

J. Kim[a]; Y. Chong[a]
[a] Department of Biosciences and Biotechnology, Konkuk University, Seoul, South Korea

To cite this Article Kim, J. and Chong, Y.(2006) 'Docking and binding mode analysis of aryl diketoacids (ADK) at the active site of HCV RNA-dependent RNA polymerase', Molecular Simulation, 32: 14, 1131 — 1138
To link to this Article: DOI: 10.1080/08927020601007538
URL: http://dx.doi.org/10.1080/08927020601007538

Molecular Simulation, Vol. 32, No. 14, 15 December 2006, 1131–1138

Taylor & Francis
Taylor & Francis Group

Docking and binding mode analysis of aryl diketoacids (ADK) at the active site of HCV RNA-dependent RNA polymerase

J. KIM and Y. CHONG*

Department of Biosciences and Biotechnology, Konkuk University, 1 Hwayang-dong, Gwangjin-gu, Seoul 143-701, South Korea

(Received July 2006; in final form September 2006)

The pharmacophore-guided docking study of aryl diketoacid (ADK) analogues revealed two distinctive hydrophobic binding sites (a pocket and a groove) around the UTP-binding site of hepatitis C virus (HCV) RNA-dependent RNA polymerase (RdRp). Interestingly, the hydrophobic binding sites have appropriate shape and size to specifically substituted aromatic rings, which suggests the specific role of substituents on the aromatic ring in determining the binding affinity of the ADK analogue to the active site of the target enzyme. Binding mode analysis of ADK analogues with potent antiviral activity shows highly substituted aromatic rings map well onto the hydrophobic binding sites. For less active compounds, their lack of aromatic substitution and thereby insufficient size can be primarily ascribed to their inability to bind to the hydrophobic binding site. The characteristic binding mode of ADK analogues proposed in this study provides a useful tool in designing a structure–activity relationship study of novel ADK analogues based on various aromatic substituents.

Keywords: Hepatitis C virus (HCV); RNA-dependent RNA polymerase; Aryl diketoacid (ADK); Docking; FlexX-pharm

1. Introduction

About 170 million people of the world population are chronically infected with hepatitis C virus (HCV), an infection that leads to liver cancer in many patients. There is neither vaccine nor effective therapy available against this pathogen, and, therefore, there is an urgent need for efficient means of combating and, ultimately, curing this viral disease. The RNA-dependent RNA polymerase (RdRp) activity of HCV protein NS5B is an absolute requirement for replication of the virus. This enzyme exhibits important differences with cellular polymerases and is therefore a good target for developing specific anti-HCV therapies [1–4]. Accordingly, in the past decade, the development of inhibitors targeting the HCV polymerase activity has attracted the attention of investigators worldwide. Not surprisingly, like other antiviral drug discovery, nucleoside analogues have led the scientific efforts in this field, and several 2′-modified nucleoside analogues with potent inhibitory activity against the HCV RdRp have been identified [5–9]. On the other hand, pyrophosphate mimics including diketo acid derivatives have emerged as novel antiviral agents. Over 200 aryl α,γ-diketo acids (ADKs) were discovered from random screening as selective inhibitors of HCV RdRp [10]. The diketo acid moiety proved essential for activity, and optimization led to the identification of an ADK inhibitor with IC_{50} value of 45 nM, one of the most potent HCV RdRp inhibitors reported. However, in spite of the remarkable antiviral activity of ADK analogues, it is not clear where this class of compounds bind on the enzyme, which limits focused structure-activity relationship studies to develop more specific and more potent inhibitor of this kind.

In this study, we designed a strategy with the aim of identifying an ADK binding site of HCV RdRp, which was then used for docking and binding mode analysis of ADKs.

2. Materials and methods

All molecular modelling of the enzyme–ligand complexes was carried out on a Linux enterprise operation system using SYBYL 7.2 software packages (Tripos Inc. St Louis, Mo, USA).

*Corresponding author. Tel.: + 82-2-2049-6100. Fax: + 82-2-454-8217. Email: chongy@konkuk.ac.kr

Molecular Simulation
ISSN 0892-7022 print/ISSN 1029-0435 online © 2006 Taylor & Francis
http://www.tandf.co.uk/journals
DOI: 10.1080/08927020601007538

2.1 UTP docking at the active site of HCV RdRp (1GX6)

Three-dimensional crystal structure of HCV RdRp was obtained from the protein data bank (PDB code 1GX6). For the docking purpose, the bound ligand (UTP) and two Mn atoms are used to define the binding pocket. The docking experiments were partly carried out with this structure, here referred to as "crystal structure", and partly using a minimized version of this protein structure, referred to as "relaxed structure", which was processed as follows: Gästeiger-Hückel charges [11,12] were given to the ligand with formal charges (+2) to two Mn atoms in the active site. Then, Kollman-All-Atom charges [13,14] were loaded to the enzyme site from the biopolymer option. The structure was then minimized using the conjugate gradient algorithm for 10,000 steps with no initial optimization, using Tripos force field [15]. The non-bonding cut-off was set to 15 A° and a distance dependent dielectric constant was applied. All atoms of the protein were treated as aggregates, with the exception of those within the 15 A° radius of the bound ligand (UTP). The ligand (UTP) was pre-processed before docking calculations by giving charges according to the Gästeiger-Hückel method followed by energy minimization with 10,000 iterations of conjugate gradient algorithm using Tripos force field. By using the FlexX module in the SYBYL 7.2 package, UTP was docked into both the crystal structure and the relaxed one. For both structures the active sites include all residues within 15 A° radius of the bound ligand and metals. Other functions were set to default values.

2.2 Generation of the ligand (ADKs) structures

Three-dimensional structures of 88 diketo acid molecules [16,17] were constructed using the sketch module in the SYBYL package, and conformational search was performed by grid search which calculates energies by systematically changing the dihedral angles of each ligand using standard Tripos force field. SYBYL computes and records molecular mechanics energies for each conformation sampled. Among them, the lowest energy structures were selected as the conformer for the FlexX and FlexX-Pharm studies. Finally all ligands were fully optimized using the standard Tripos force field with Gästeiger-Hückel charges until the energy gradient converged to below 0.05 kcal/mol.

2.3 Generation of the pharmacophore constraints for FlexX-pharm study

On the basis of several X-ray structures of viral polymerases, it is known that the triphosphate binding pocket is highly conserved. Two divalent metal ions are tightly held by active site residues containing aspartic acid side chains, which, in turn, electrostatically interact with phosphate oxygen atoms. The triphosphate moiety becomes further stabilized by neighbouring amino acid residues. In HCV RdRp, Asp225 and Phe224 are heavily involved in this stabilizing interaction. Thus, for a ligand to bind to the active site of HCV RdRp, this interaction is prerequisite. For the purpose of virtual screening, this was considered an essential interaction, and the docking of the ADKs was biased to ensure that these electrostatic interactions were satisfied by specifying that interactions be made with two Mn atoms, the backbone NH of Phe224 and Asp225. Investigation of the X-ray structure of UTP bound to the HCV RdRp reveals that the polypeptide main chain around Leu159 can serve as both hydrogen bonding donor (amide backbone —NH) and acceptor (amide carbonyl C═O). To account for this, docking of compounds was guided by having essential interactions with the polypeptide main chain of Leu159, but optional in choosing backbone NH or backbone carbonyl for the hydrogen bonding partner.

2.4 Docking with FlexX and FlexX-pharm

Active site of the enzyme was defined as all the residues within 15 A° of the bound ligand and two metal ions. Standard parameters were used as implemented in SYBYL 7.2 package. Formal charges and the particle concept options were always checked. In each case, a maximum of 100 poses were saved for each docked compound, although typically many fewer (30 poses) were saved because biased sampling was used in the docking process.

3. Results

3.1 Self-docking of UTP at the active site of HCV RdRp

In order to understand the characteristic binding modes of ADKs, we tried to find a rational way to locate the ligands at the active site of HCV RdRp, which has rarely been tried presumably due to the difficulties in treating the RNA (or DNA) duplex in calculation. In the case of non-nucleoside viral polymerase inhibitors, however, RNA duplex does not come into play and, as a result, virtual screening study becomes feasible. A crystal structure of HCV RdRp bound with UTP at the active site in the absence of RNA (1GX6) provides an appropriate platform for this purpose. Water molecules and the ligand (UTP) were removed to generate the enzyme site, which was energy-minimized to mimic the conformation of the free enzyme. The docking experiment was conducted by using the FlexX release 2. Fitting UTP of the crystal structure and the one docked into the relaxed structure resulted in an RMS deviation of 0.819 A°, which shows that the docked pose of UTP does not differ significantly from the crystal structure (figure 1). Thus, as expected, it looks like that generation of the binding mode of a ligand can be generated by docking the ligand at the active site of HCV RdRp.

3.2 Analysis of binding mode of UTP to the HCV RdRp

The finding that UTP binds at the catalytic site with the base hydrogen bonded to the polypeptide main chain is,

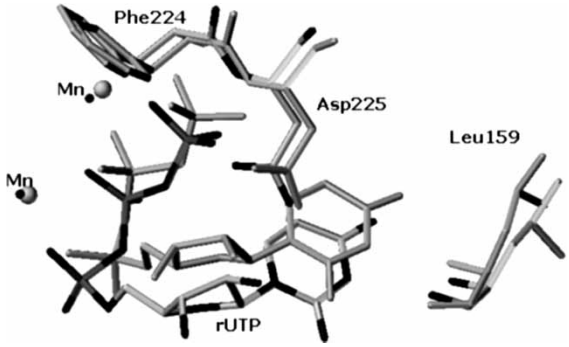

Figure 1. Comparison of the UTP-binding site of the crystal structure (black and white) and self-docking structure (grey).

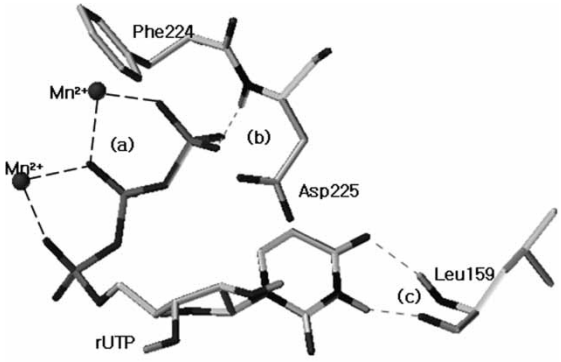

Figure 2. Pharmacophore model of UTP including the key binding interactions between UTP and HCV RdRp: (a) electrostatic interaction between Mn^{2+} and phosphate; (b) H-bonding between Phe224 and phosphate; (c) H-bonding between uracil base and Leu159.

although artificial in the sense that UTP cannot bind in such a way in the presence of template, important for the conception of new specific antiviral drugs. Analysis of the crystal structure reveals a pharmacophore model of UTP which includes three key interactions with HCV RdRp, i.e. (i) electrostatic interaction between two divalent metal ions and the triphosphate moiety, (ii) stabilization of the triphosphate moiety by polypeptide NH backbone of Phe224 and Asp225, (iii) hydrogen bonding of the uracil base with backbone NH as well as backbone carbonyl of Leu159 (figure 2).

3.3 Structural comparison of UTP with ADK

As the pharmacophore model of UTP shows, the most important feature of a ligand which binds to the active site of HCV RdRp either in the presence or absence of RNA duplex is chelation of two divalent metal ions. In this regard, it is noteworthy that ADK is generally considered to be a good metal chelator through its diketo acid functionality [18,19]. Interestingly, when the metal-chelating groups were allowed to overlap atom by atom, hydrogen bonding donor (NH) and acceptor (CO) of the uracil base of UTP were found to be in perfect match with the corresponding donor (NH) and acceptor (SO_2) of one of the ADK molecule (**1**) (figure 3). Thus, it is conceivable that ADK analogues have the same pharmacophore as UTP and might be able to bind at the catalytic site of HCV RdRp by the similar fashion as UTP in the absence of RNA duplex.

3.4 Docking ADKs into the active site of HCV RdRp

Molecular docking programs face several challenges in trying to predict correctly the binding mode of a protein-inhibitor complex. In general, the top pose identified fails to regenerate the key interaction found in the crystal structure. Docking with FlexX into the active site of HCV RdRp almost every ADK molecules were successfully docked. However, the top pose did not show any specific interaction with enzyme residues other than electrostatic interaction with Mn^{2+} ion, which significantly restricted the docking protocol in understanding the common binding mode of ADK analogues.

In FlexX-Pharm [20], which is an extended version of FlexX, a previously defined set of pharmacophore features in the active site constraints the docking calculation so that only solutions are produced that match the specified set of features. For docking with FlexX-Pharm, interacting groups and the corresponding interaction type (hydrogen bond donor, acceptor, hydrophobic pocket) in the active site must be specified. FlexX-Pharm then ensures that an interaction is formed between the specified interaction group in the active site and the ligand in a valid docking solution. During docking, the set of pharmacophore constraints is used to guide the construction of the ligand in the active site, ensuring that undesirable partial solutions are filtered out early in the course of the calculation. The result is a focused set of docked solutions

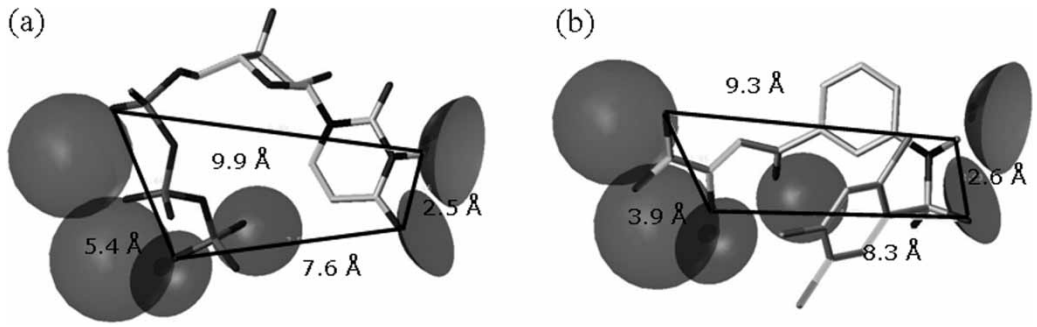

Figure 3. Comparison of the pharmacophores of (a) UTP and (b) ADK (**1**). Grey dishes indicate specific interactions around the pharmacophore with the amino acid residues: electrostatic interaction with divalent metal ions (left two dishes), H-bond acceptors (bottom three dishes), and H-bond donors (right).

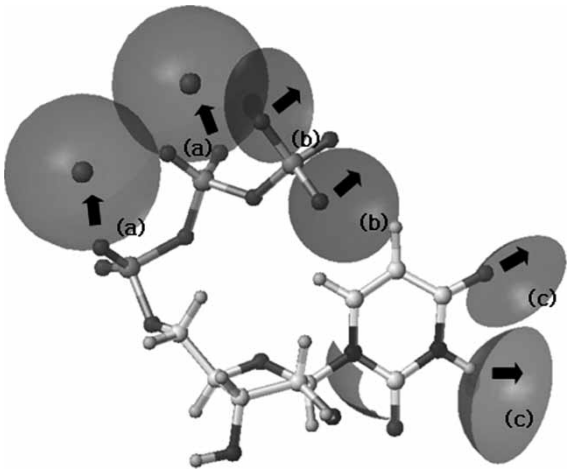

Figure 4. Most critical interactions between ligand and HCV RdRp used as guidelines for docking by FlexX-Pharm: (a) Electrostatic interaction with Mn^{2+}; (b) H-bonding with Phe224 and Asp225; and (c) H-bonding with Leu159. Grey dishes indicate UTP-binding site of the enzyme characterized by these conditions.

and a speed-up in the calculation. This methodology leads to a more intensive search of the conformational space defined by the pharmacophore constraints, increasing the opportunity for novel docked solutions to appear.

In order to find out if ADK molecules could have the same binding mode as UTP, 88 ADK molecules with known IC_{50} values [16,17] were docked into the active site of HCV RdRp by using the FlexX-Pharm programs of SYBYL 7.2. For docking with FlexX-Pharm the most critical interactions between ligands and HCV RdRp, i.e. electrostatic interactions to divalent Mn^{2+}, and H-bridges to three amino acid residues (Phe224, Asp225 and Leu159) were mapped in the crystal structure (figure 4).

It should be noted that, for the sake of filtering the ligands with non-specific binding interactions, H-bridge to the Leu159 was included in a set of pharmacophore constraints. Among 88 ADK analogues screened, only 23 molecules were successfully docked (table 1, figure 5).

Table 1. Biological activity (IC_{50}) of ADK analogues [18,19].

Compound	*IC_{50} (μM)*
1	0.049
2	0.056
3	0.10
4	0.10
5	0.11
6	0.14
7	0.67
8	0.95
9	1.0
10	4.6
11	6.0
12	6.3
13	7.6
14	8.0
15	13.0
16	13.0
17	17.0
18	19.0
19	19.0
20	27.0
21	40.0
22	50.0
23	50.0

Not surprisingly, these molecules include phenolic or anilinic derivatives as their aromatic moieties of which oxygen or nitrogen atoms are involved in hydrogen bonding with the amide backbone of Leu159.

3.5 Analysis of binding modes of ADKs to the HCV RdRp

Analysis of the top poses of the enzyme–ligand complexes shows that hydrophobic interaction between the aromatic moiety of the ligand and the enzyme is another key player in determining the binding affinity. The U-shaped channel provides two hydrophobic binding sites for the aromatic moieties of ADK molecules (figure 6). One is a hydrophobic pocket around Leu159 which is lined up with eight amino acid residues (Tyr4, Trp6, Gln49, Ile138, Ile159, Val161, Asp225 and Arg280) and the other is a shallow groove located at the bottom of a U-shape channel (Arg48, Lys51, Val52, Arg158 and Cys223) (figure 6).

Most ADK analogues were docked into the hydrophobic pocket (figure 6) with the phenolic oxygen or anilinic nitrogen atoms served as hydrogen bond acceptors which interact with backbone NH of Leu159. However, sulfonamide derivatives (**1**, **6**), which have both hydrogen bond donor and acceptor in a sulfonamide moiety, showed different binding modes and their aromatic rings were positioned on the hydrophobic groove instead of the pocket (figure 6). The sulfonamide would act as a hydrogen-bonding donor to interact with the backbone carbonyl oxygen instead of backbone NH of Leu159. The slight difference in hydrogen bonding interaction determines the location of the aromatic moieties of the ADK molecules, either into the hydrophobic pocket or on the groove. It should be noted that both hydrophobic surfaces (pocket and groove) are large enough to accommodate substituted aromatic rings, which can stabilize the bound ADK analogues through extensive van der Waals interaction. The hydrophobic pocket is of another great interest due to its characteristic structure (figure 7). The pocket has an excellent three-dimensional arrangement to accommodate substituted aromatic compounds (figure 7a). Particularly, a hydrophobic hole deep inside the pocket which is composed of side chains of Trp6, Val161, Ile138 and Gln49 provides perfect size for binding a chlorine or bromine atom (figure 7b).

ADK analogues with substituted aromatic rings such as **2**, **3**, **4** and **7** bind to this specific hydrophobic pocket and show high biological activity (IC_{50} values 0.056, 0.10, 0.10 and 0.67 μM, respectively). However, compound **14** which has a non-substituted aromatic ring shows a very loose binding mode at the hydrophobic pocket which results in a significant decrease in activity (IC_{50}, 8.0 μM, figure 8).

On the other hand, hydrogen bonding donors such as sulfonamides **1** and **6** locate their aromatic rings at the

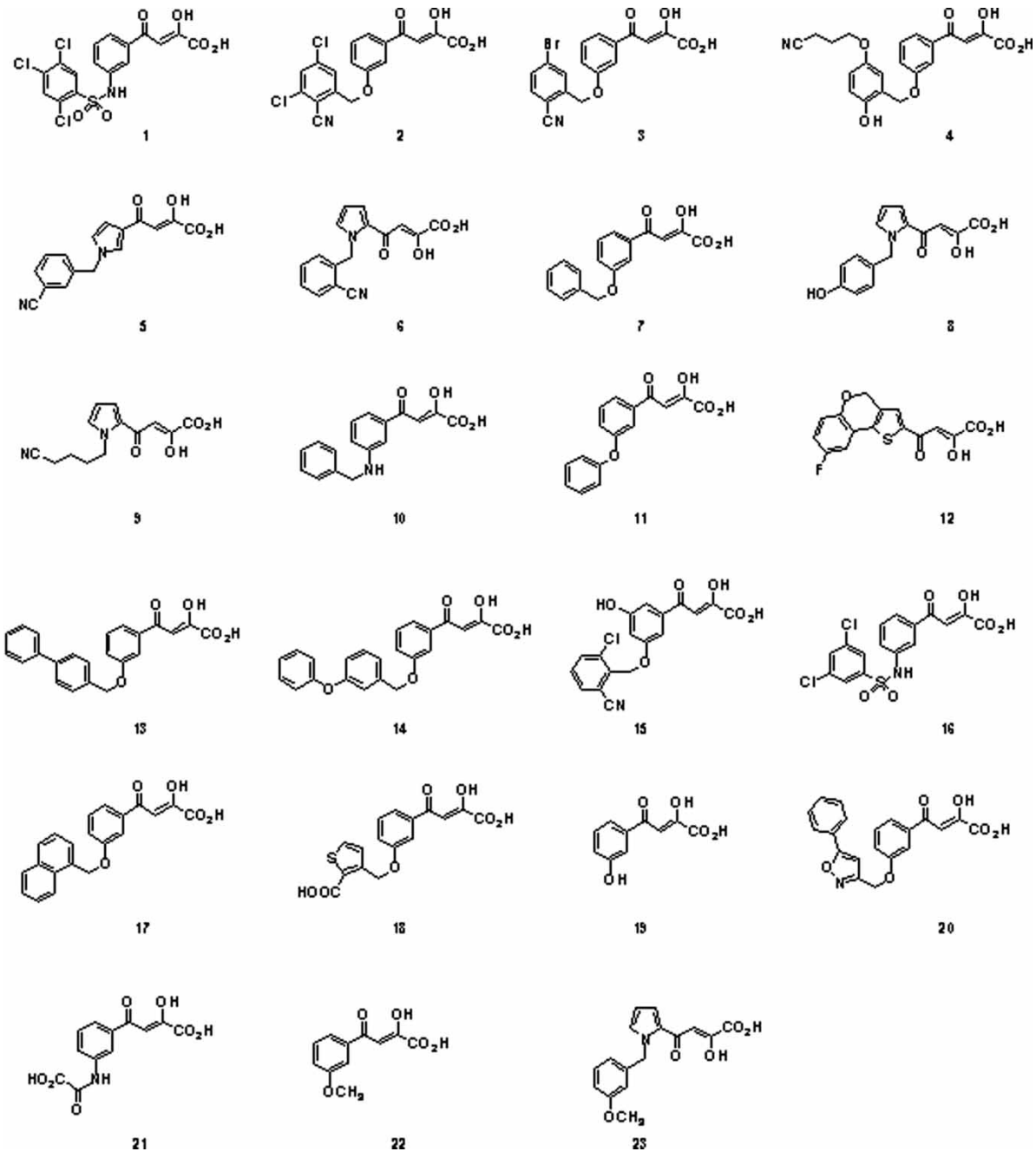

Figure 5. Twenty three ADK analogues successfully docked at the UTP-binding site of HCV RdRp by FlexX-Pharm docking method.

bottom of the groove which connects the hydrophobic channel with the surface of the enzyme. This groove is shown blocked in the crystal structure of HCV RdRp without bound ligand (1QUV, [1]) but upon binding UTP, two arginine residues (Arg48, Arg158) rotate away to provide room for the ligand (1GX6). The groove, thus formed, is also well organized to accommodate substituted aromatic rings (figure 9). Particularly, two small holes at the end of the groove provide excellent matches with the size of chlorine or bromine atom. Two sulfonamide ADK analogues (**1**, **6**) possess aromatic substituents with comparable size to the groove, which results in high biological activity (IC_{50} values 0.049, 0.14, μM, respectively).

4. Discussion

Several interesting structural features were revealed through analysis of the HCV RdRp crystal structure. Among the unique features, HCV RdRp includes an encircled active site with an overall globular shape instead of the typical U-shape found in other polymerases [1–4]. As a result, HCV RdRp is unlikely to open up upon binding of the RNA template/primer complex, as, for example, in the case for HIV reverse transcriptase [21]. Thus, although none of the crystal structures of HCV RdRp was solved with RNA or metal ions bound to the active site, those structures could be used as a template for the structure-based inhibitor design study because the

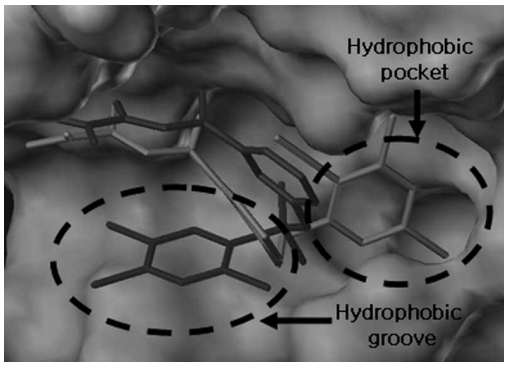

Figure 6. Two different hydrophobic binding sites of HCV RdRp. ADK analogues **1** and **2** are shown in dark and light grey, respectively. Hydrophobic pocket around light grey aromatic ring is indicated by dotted circle. Hydrophobic groove below dark grey aromatic ring is also indicated by dotted circle.

superimposable structures might represent catalytically competent conformations of the active site of the enzyme.

In this respect, as Bressanelli *et al.* have noted [2], the finding that UTP binds to HCV RdRp with the base (uracil) hydrogen bonded to the polypeptide main chain (PDB code 1GX6) provides an interesting implication for designing new specific antiviral drugs. This alternative-binding mode of UTP is artificial in the sense that UTP cannot bind in such a way in the presence of template, but it is conceivable that molecules with higher binding affinity to the UTP-binding site in this mode can inhibit the catalytic activity of the enzyme. For this purpose, we set out to investigate the characteristic binding mode of UTP and constructed a pharmacophore model composed of three key interactions of UTP with HCV RdRp (figure 2): (a) electrostatic interaction with two divalent metal ions (Mn^{2+}), (b) H-bonding of triphosphate moiety to nearby amino acid residues (Phe224, Asp225), and (c) H-bonding between uracil base and Leu159. The generated pharmacophore has an interesting match with ADK of which diketo acid moiety and H-bond donor/acceptor are in good three-dimensional agreements with the triphosphate and uracil base of the UTP, respectively (figure 3). Therefore, ADK analogues share the similar structural features with UTP for binding to the same site of the HCV

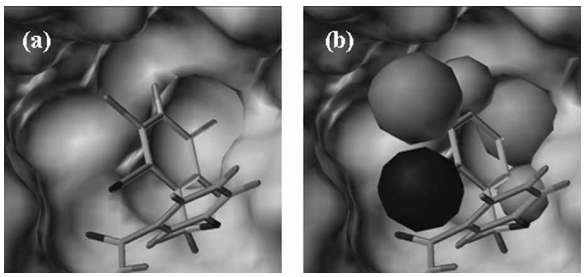

Figure 7. Hydrophobic pocket around Leu159: (a) the pocket is in perfect shape and size for accommodation of substituted aromatic ring. The lumpy bright surface around the ADK molecule indicates a hydrophobic binding site, which includes a deep and shallow hydrophobic hole at the center; and (b) a shallow hydrophobic hole deep inside the pocket has a room for bulky atoms such as chlorine or bromine. The chlorine atom rendered as a ball and stick model is snuggly fitted into the hole.

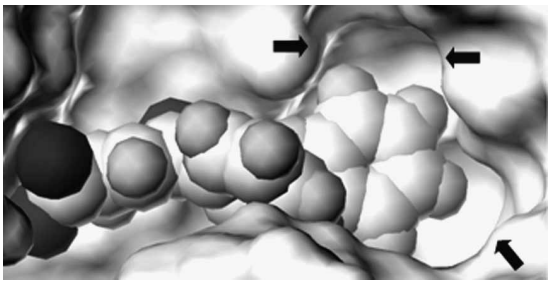

Figure 8. Compound **14** docked at the UTP-binding site of HCV RdRp: Non-substituted aromatic ring does not fit into the hydrophobic pocket due to the lack of hydrophobic interaction. Hydrophobic pocket is shown by arrows.

RdRp (figure 3). In other words, although ADK interacts with divalent metal ions, its binding site might be distinct from the substrate-binding site of HCV RdRp. In this regard, it is noteworthy that the mechanism of action of ADK and related compounds was found to be non-competitive with respect to both the RNA template and to the nucleotides [22]. Due to the capability of ADKs to interact directly with the catalytic metal ions found in the enzyme active site [18,19], they can be considered as product-like inhibitors showing a mechanism of action similar to that of Foscarnet, a known pyrophosphate analogue. Through noncompetitive inhibition, Foscarnet blocks the pyrophosphate binding site of viral DNA polymerase, thereby preventing the cleavage of pyrophosphate from deoxynucleoside triphosphate and elongation of the viral DNA chain. However, differently substituted ADKs were characterized, with each inhibiting HIV-1 RT or HBV polymerases in a highly selective manner [17] whereas Foscarnet shows broad-spectrum anti-herpes virus activity. Thus, it is conceivable that the selectivity of ADKs might come from its aromatic substituents and, by the same token, HCV RdRp might have additional characteristic binding site other than the pyrophosphate binding sites to selectively accommodate the ADKs with various aromatic substituents. The contribution of the aromatic rings of ADKs to their binding affinity was confirmed by Di Santo *et al.* [16]. They constructed a 3D chemical-feature-based pharmacophore model, which consisted of two hydrogen bond acceptors, one negative ionizable moiety, and two hydrophobic aromatics.

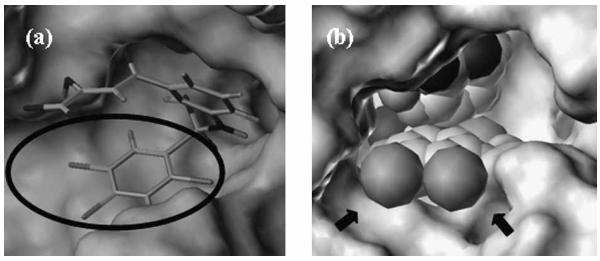

Figure 9. Interaction between aromatic ring of ADK (**1**) and hydrophobic groove: (a) Top view. Hydrophobic groove is located at the opposite side of the pocket (circle). (b) Side view. Hydrophobic groove becomes hollow at the end of the channel to provide excellent binding sites for bulky atoms such as chlorine and bromine. The hydrophobic holes are shown by arrows.

The pharmacophore model provided invaluable insights into the structural requirements for ADK analogues to be active against HCV RdRp. However, in spite of a high correlation coefficient ($r = 0.965$), the pharmacophore model did not provide detailed binding modes of ADKs which are required for designing more potent ADK analogues by various aromatic substituents [16].

Based on these findings, we attempted to construct a binding model of ADK molecules by postulating that ADKs bind to the HCV RdRp via electrostatic interaction with divalent metal ions as well as H-bonding with amino acid residues (Phe224, Asp225, Leu159). Also, we assumed that there might be an additional binding site which is specific for aromatic substituents of ADKs.

The binding mode analysis of viral polymerase inhibitors has been hampered presumably due to the computational difficulties in dealing with a complicated enzyme-RNA duplex-ligand ternary complex system. The advantage of the non-nucleoside noncompetitive inhibitors is that the RNA duplex does not need to be considered in docking study. Therefore, we were able to regenerate the UTP binding mode of the crystal structure (1GX6) with significant accuracy by docking of UTP to the relaxed structure of HCV RdRp. Pharmacophore-guided docking (FlexX-Pharm) study of ADK molecules provided two hydrophobic binding sites (a pocket and a groove) which have excellent three dimensional arrangements to accommodate substituted aromatic rings (figures 6–9) in addition to the metal binding site and H-bonding site in the polypeptide chain of HCV RdRp. Interestingly, both of the hydrophobic binding sites have holes with a size comparable to chlorine and bromine atoms, which accounts for potent antiviral activity of ADK analogues with chlorine- or bromine-substituted aromatic rings. Thus, through comparison of binding modes of potent ADK analogues with those of less potent ones, it became clear how aromatic substituents contribute to the binding of ADKs to the target enzyme. More importantly, the characteristic binding modes of ADK analogues proposed in this study provides a useful tool in designing an extensive structure–activity relationship study of novel ADK analogues based on various aromatic substituents.In summary, the pharmacophore-guided docking study revealed two distinctive hydrophobic binding sites around the UTP-binding site of HCV RdRp, which have appropriate shape and size for specific binding of substituted aromatic rings. The ADK analogues with highly substituted aromatic rings (**1** ∼ **4**), which show potent antiviral activity, map well onto the hydrophobic binding sites to reinforce the hydrophobic interaction with the target enzyme. For less active compounds, their lack of aromatic substitution and thereby insufficient size can be primarily ascribed to their inability to bind to the hydrophobic binding site.

Acknowledgements

This work was supported by the Korea Research Foundation Grant funded by the Korean Government (MOEHRD, Basic Research Promotion Fund) (KRF-2006-003-C00176), by a grant Biogreen 21 (Korea Ministry of Agriculture and Forestry) and the second Brain Korea 21 (Korea Ministry of Education). Jinyoung Kim is supported by the second Brain Korea 21.

References

[1] H. Ago, T. Adashi, A. Yoshida, M. Yamamoto, N. Habuka, K. Yatsunami, M. Miyano. Crystal structure of the RNA-dependent RNA polymerase of hepatitis C virus. *Structure*, **7**, 1417 (1999).

[2] S. Bressanelli, L. Tomei, F.A. Rey, R. De Francesco. Structural analysis of the hepatitis C virus RNA polymerase in complex with ribonucleotides. *J. Virol.*, **76**, 3482 (2002).

[3] S. Bressanelli, L. Tomei, A. Roussel, I. Incitti, R.L. Vitale, M. Mathieu, R. De Francesco, F.A. Rey. Crystal structure of the RNA-dependent RNA polymerase of hepatitis C virus. *Proc. Natl. Acad. Sci. USA*, **96**, 13034 (1999).

[4] C.A. Lesburg, M.B. Cable, E. Ferrari, Z. Hong, A.F. Mannarino, P.C. Weber. Crystal structure of the RNA-dependent RNA polymerase from hepatitis C virus reveals a fully encircled active site. *Nat. Struct. Biol.*, **6**, 937 (1999).

[5] L.J. Stuyver, T.R. McBrayer, T. Whitaker, P.M. Tharnish, M. Ramesh, S. Lostia, L. Cartee, J. Shi, A. Hobbs, R.F. Schinazi, K.A. Watanabe, M.J. Otto. Inhibition of the subgenomic hepatitis C virus replicon in huh-7 cells by 2′-deoxy-2′-fluorocytidine. *Antimicrob. Agents Chemother.*, **48**, 651 (2004).

[6] L.J. Stuyver, T.R. McBrayer, P.M. Tharnish, A.E. Hassan, C.K. Chu, K.W. Pankiewicw, K.A. Watanabe, R.F. Schinazi, M.J. Otto. Dynamics of subgenomic hepatitis C virus replicon RNA levels in Huh-7 cells after exposure to nucleoside antimetabolites. *J. Virol.*, **77**, 10689 (2003).

[7] A.B. Eldrup, C.R. Allerson, C.F. Bennett, S. Bera, B. Bhat, N. Bhat, M.R. Bosserman, J. Brooks, C. Burlein, S.S. Carroll, P.D. Cook, K.L. Getty, M. MacCoss, D.R. McMasters, D.B. Olsen, T.P. Prakash, M. Prhavc, Q. Song, J.E. Tomassini, J. Xia. Structure–activity relationship of purine ribonucleosides for inhibition of hepatitis C virus RNA-dependent RNA polymerase. *J. Med. Chem.*, **47**, 2283 (2004).

[8] A.B. Eldrup, M. Prhavc, J. Brooks, B. Bhat, T.P. Prakash, Q. Song, S. Bera, N. Bhat, P. Dande, P.D. Cook, C.F. Bennett, S.S. Carroll, R.G. Ball, M. Bosserman, C. Burlein, L.F. Colwell, J.F. Fay, O.A. Flores, K. Getty, R.L. Lafemina, J. Leone, M. MacCoss, D.R. McMasters, J.E. Tomassini, D. VonLangen, B. Wolanski, D.B. Olsen. Structure–activity relationship of heterobase-modified 2′-C-methyl ribonucleosides as inhibitors of hepatitis C virus RNA replication. *J. Med. Chem.*, **47**, 5284 (2004).

[9] J.L0. Clark, L. Hollecker, J.C. Mason, L.J. Stuyver, P.M. Tharnish, S. Lostia, T.R. McBrayer, R.F. Schinazi, K.A. Watanabe, M.J. Otto, P.A. Furman, W.J. Stec, S.E. Patterson, K.W. Pankiewicz. Design, synthesis, and antiviral activity of 2′-deoxy-2′-fluoro-2′-C-methyl-cytidine, a potent inhibitor of hepatitis C virus replication. *J. Med. Chem.*, **48**, 5504 (2005).

[10] V. Summa, A. Petrocchi, P. Pace, V.G. Matassa, R. De Francesco, S. Altamura, L. Tomei, W. Koch, P. Neuner. Discovery of α, γ-diketo acids as potent selective and reversible inhibitors of hepatitis C virus NS5B RNA-dependent RNA polymerase. *J. Med. Chem.*, **47**, 14 (2004).

[11] J. Gästeiger, M. Marsili. Iterative partial equalization of orbital electronegativity—A rapid access to atomic charges. *Tetrahedron*, **36**, 3219 (1980).

[12] W.P. Purcell, J.A. Singer. A brief review and table of semiempirical parameters used in the Hückel molecular orbital method. *J. Chem. Eng. Data.*, **12**, 235 (1967).

[13] J.M. Blaney, P.K. Weiner, A. Dearing, P.A. Kollman, E.C. Jorgensen, S.J. Oatley, J.M. Burridge, C.C.F. Blake. Molecular mechanics simulation of protein–ligand interactions: binding of thyroid hormone analogs to prealbumin. *J. Am. Chem. Soc.*, **104**, 6424 (1982).

[14] G. Wipff, A. Dearing, P.K. Weiner, J.M. Blaney, P.A. Kollman. Molecular mechanics studies of enzyme–substrate interactions: the interaction of L- and D-*N*-acetyltryptophanamide with α-chymotrypsin. *J. Am. Chem. Soc.*, **105**, 997 (1983).

[15] K.M. Gilbert, W.J. Skawinski, M. Misra, K.A. Paris, N.H. Naik, R.A. Buono, H.M. Deutsch, C.A. Venanzi. Conformational analysis of methylphenidate: comparison of molecular orbital and molecular mechanics methods. *J. Comput. Aided Mol. Des.*, **18**, 719 (2004).

[16] R. Di Santo, M. Fermeglia, M. Ferrone, M.S. Paneni, R. Costi, M. Artico, A. Roux, M. Gabriele, K.D. Tardif, A. Siddiqui, S. Pricl. Simple but highly effective three-dimensional chemical–feature-based pharmacophore model for diketo acid derivatives as hepatitis C virus RNA-dependent RNA polymerase inhibitors. *J. Med. Chem.*, **48**, 6304 (2005).

[17] S. Altamura, L. Tomei, U. Koch, P.J. Neuner, V. Summa. Diketoacid-derivatives as inhibitors of polymerases. *PCT Int. Appl.*, WO 2000006529 (2000).

[18] J.A. Grobler, K. Stillmock, B. Hu, M. Witmer, P. Felock, A.S. Espeseth, A. Wolfe, M. Egbertson, M. Bourgeois, J. Melamed. Diketo acid inhibitor mechanism and HIV-1 integrase: implications for metal binding in the active site of phosphotransferase enzymes. *Proc. Natl. Acad. Sci. USA*, **99**, 6661 (2002).

[19] G.C. Pais, X. Zhang, C. Marchand, N. Neamati, K. Cowansage, E.S. Svarovskaia, V.K. Pathak, Y. Tang, M. Nicklaus, Y. Pommier. Structure activity of 3-aryl-1, 3-diketo-containing compounds as HIV-1 integrase inhibitors. *J. Med. Chem.*, **45**, 3184 (2002).

[20] S.A. Hindle, M. Rarey, C. Buning, T. Lengaue. Flexible docking under pharmacophore type constraints. *J. Comput. Aided Mol. Des.*, **16**, 129 (2002).

[21] H. Huang, R. Chopra, G. Verdine, S.C. Harrison. Structure of a covalently trapped catalytic complex of HIV-1 reverse transcriptase: implications for drug resistance. *Science*, **282**, 1669 (1998).

[22] R. De Francesco, L. Tomei, S. Altamura, V. Summa, G. Migliaccio. Approaching a new era for hepatitis C virus therapy: inhibitors of the NS3-4A serine protease and the NS5B RNA-dependent RNA polymerase. *Antiviral Res.*, **58**, 1 (2004).